

Maximising Manipulability During Resolved-Rate Motion Control

Jesse Haviland¹, Peter Corke¹

Abstract—Resolved-rate motion control of redundant serial-link manipulators is commonly achieved using the Moore-Penrose pseudoinverse in which the norm of the control input is minimized. However, as kinematic singularities are a significant issue for robotic manipulators, we propose a Manipulability Motion Controller which chooses joint velocities which will also increase the manipulability of the robot. The manipulability measure has a complex non-linear relationship with the robot’s joint configuration and in this paper we derive the manipulability Jacobian which directly relates joint velocities to the rate of change of manipulability. Furthermore, we use the manipulability Jacobian within a constrained quadratic program to create an improved resolved-rate motion controller for redundant robots. The resulting real-time controller provides joint velocities which achieve a desired Cartesian end-effector velocity while also maximising the robot’s manipulability. We illustrate and verify our control scheme on several popular serial-link manipulators and provide an open-source library which implements our controller (available at [jhavl.github.io/mmc](https://github.com/jhavl/mmc)).

I. INTRODUCTION

Being robust and reactive is a significant challenge for serial-link manipulators. Progress towards this goal comes from more capable robots, improved perception of the environment, and a better understanding of the robot’s kinematic constraints. However, many proposed solutions to these issues often reduce the reactivity of the system due to computational load.

The forward kinematics of a serial-link manipulator provides a non-linear mapping from its joint space to its Cartesian task space. The non-linearity makes it difficult and computationally expensive to solve robotic motion problems in terms of joint configuration and Cartesian positions, which results in a less reactive controller.

However, by taking the derivative of the robot kinematics, the problem becomes linear (at the instant of the robot’s current joint configuration). This approach, where the end-effector velocity is directly related to the joint velocity through the kinematic Jacobian, is the well known and classic approach called resolved-rate motion control.

Resolved-rate motion control allows for direct control of the robot’s end-effector velocity, without expensive path planning. Consequently, it is well-suited to reactive control schemes such as visual servoing. Modern manipulators are typically redundant, 7 DoF is the new normal, and classical resolved-rate motion control cannot exploit this new capability.

¹Jesse Haviland and Peter Corke are with the Australian Centre for Robotic Vision (ACRV), Queensland University of Technology Centre for Robotics (QCR), Brisbane, Australia j.haviland@qut.edu.au, peter.corke@qut.edu.au. This research was conducted by the Australian Research Council project number CE140100016, and supported by the QUT Centre for Robotics.

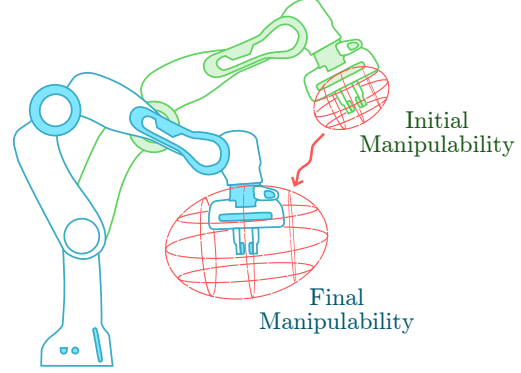


Fig. 1: Our Manipulability Motion Controller drives a redundant robot’s joint velocities such that the manipulability of the robot is maximised, while achieving the desired end-effector velocity. The manipulability can be visualised through velocity ellipsoids created using the kinematic Jacobian (more details in Figure 2).

Redundant manipulators have more degrees of freedom than is necessary to reach any pose within their task space. Consequently, the robot can achieve any task space pose with an infinite number of joint configurations (subject of course to reachability and joint limits). The challenge is then to introduce constraints in order to choose the “best” joint configuration to achieve the pose. Serial-link manipulators are also subject to joint limits and kinematic singularities (joint configurations where the robot’s task space is reduced by one or more degrees of freedom).

A measure of manipulability, devised in [1], describes how well-conditioned the manipulator is to achieve any arbitrary velocity. The measure provides a single scalar value which represents the volume of a 6-dimensional velocity ellipsoid. This measure indicates how close the manipulator’s configuration is to a singularity. Therefore, maximising the manipulability of the manipulator, as demonstrated by our controller in Figure 1, will greatly improve the velocity performance and keep the robot well away from a singularity.

The contributions of this paper are:

- 1) our Manipulability Motion Controller which controls a redundant robotic system to achieve a Cartesian velocity while maximising its manipulability.
- 2) experimental validation in simulation with several popular serial link manipulators
- 3) experimental validation on a Franka-Emika Panda robot arm
- 4) an open-source Python library which implements our controller on any serial-link manipulator

II. RELATED WORK

The goal, when kinematically controlling serial-link manipulator, is to find a control which provides the desired end-effector motion in the manipulator's task space. There is a linear mapping between the instantaneous end-effector spatial velocity and the joint velocities given by the kinematic Jacobian which is a $6 \times n$ matrix and where n is the number of robot joints. For a robot where $n = 6$ the Jacobian is square and if invertible can be used to map task space velocity to joint space velocity. This technique is the standard approach for reactive kinematic control in the velocity domain and is known as resolved-rate motion control [2].

However, if $n > 6$, the kinematic Jacobian is not square and consequently, the inverse is not possible. There are an infinite number of joint velocity vectors which will give rise to any task space velocity. We commonly use the Moore-Penrose pseudoinverse which yields the joint space velocity with the minimum Euclidean norm. Some early work used fuzzy logic to approximate the pseudoinverse which, at the time, was computationally expensive to compute in a low-level control algorithm [3].

If the condition number of the Jacobian is high, or the square Jacobian is singular, then some task-space velocities are unachievable or only achievable with very high joint velocities [4]. This has led to several approaches which use optimisation strategies for redundant manipulators.

Quadratic programs are an influential and highly used tool in optimisation. The advantage of quadratic programs lies in the fact that they can represent complex systems while always being solvable in a finite time (or shown to be infeasible) [5]. Quadratic programming, in general, can incorporate equality, inequality, and bound constraints simultaneously.

The pseudoinverse can be modelled as a quadratic programming problem. In contrast to non-linear programming, the objective function used in a quadratic programming problem is convex (under certain conditions, see Section IV) [5]. Therefore, a unique solution exists and can always be found. From a quadratic programming perspective, the pseudoinverse solution minimises the control input, in terms of joint velocity. However, this solution does nothing to stop the robot from reaching a singular position.

More recent work on kinematic control of redundant manipulators uses a planning based paradigm [6], [7]. In motion planning, joint motion is generated for the entire movement from the robot's starting pose to the goal. Recent progress in this area has seen the kinematic motion planning problem solved using techniques such as quadratic programming and neural networks.

Quadratic programming has been found to be a useful tool in motion planning for kinematic control. In [8], quadratic programming was used to aid in obstacle avoidance with redundant manipulators while in [9] it was used to maximise manipulability.

Neural networks have also been utilised for motion planning with redundant manipulators. The work in [10] used a

dynamic neural network to choose joint velocities which increase manipulability, while also staying within the physical joint limits of the robot. This is similar to the work in [11]–[14], however, the controllers devised in these works do not optimise for manipulability.

The problem with motion planning solutions is that they do not provide the level of reactivity required for control techniques such as visual servoing [15]. Purely reactive controllers, including visual servoing schemes, need direct control of the end-effector velocity as the goal information is updated on each iteration of the vision control loop. A consequence of the reactivity is that such schemes typically have not had access to the benefits of the planning based methods outlined above. Recent work completed in [16], incorporated the physical joint limits of a mobile manipulator into a quadratic programming function. However, it does not assist the robot in avoiding singularities or maximising manipulability.

In this paper, we propose a novel real-time resolved-rate motion controller which maximises the manipulability of a serial-link manipulator in a purely reactive manner. Our controller provides benefits previously only obtained through planning based methods.

In Section III we outline the traditional approach to resolved-rate motion and then relate this to a quadratic programming problem in IV. Section V details the manipulability Jacobian before we use it to formulate the proposed Manipulability Motion Controller in Section VI. Section VII describes our experimental setup and methodology. Finally, Section VIII details our experimental results and insights informed by the results.

III. RESOLVED-RATE MOTION CONTROL

The forward kinematics of a serial-link manipulator provides a non-linear surjective mapping between the joint space and Cartesian task space. This mapping is described as

$$\mathbf{r}(t) = f(\mathbf{q}(t)) \quad (1)$$

for an n DoF manipulator with n joints, where $\mathbf{q}(t) \in \mathbb{R}^n$ are the joint coordinates of the robot, $\mathbf{r} \in \mathbb{R}^m$ is some parameterization of the end-effector pose, and the mapping function $f(\cdot)$ holds the geometrical information of the robot. The following derivations assume the robot has a task space $\mathcal{T} \in \mathbf{SE}(3)$, and therefore $m = 6$. A redundant manipulator has a joint space dimension that exceeds the workspace dimension, i.e. $n > 6$. Taking the time derivative of (1)

$$\dot{\mathbf{r}}(t) = \mathbf{J}(\mathbf{q}(t))\dot{\mathbf{q}}(t) \quad (2)$$

where $\mathbf{J}(\mathbf{q}(t)) = \frac{\partial f(\mathbf{q})}{\partial \mathbf{q}} \big|_{\mathbf{q}=\mathbf{q}_0} \in \mathbb{R}^{6 \times n}$ is the manipulator Jacobian for the robot at configuration \mathbf{q}_0 . Resolved-rate motion control is an algorithm which maps a Cartesian end-effector velocity $\dot{\mathbf{r}}$ to the robot's joint velocity $\dot{\mathbf{q}}$. Through rearranging (2), the required joint velocities can be calculated as [4]

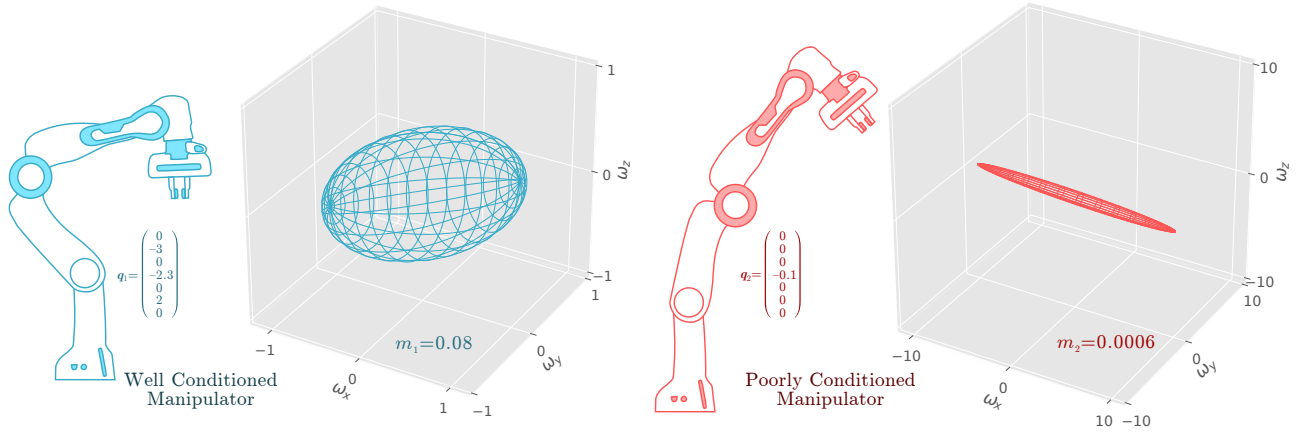


Fig. 2: End-effector angular velocity ellipsoids created using the kinematic Jacobian at two different robot configurations q_1 and q_2 , on a Panda robot. The ellipsoid depicts how easily the robot's end-effector can move with an arbitrary angular velocity. The left ellipsoid shows the manipulator's configuration is well conditioned to rotate the end-effector in any direction. The right configuration is near singular as the end-effector will struggle to rotate around the y or z-axis. This ability to move is encapsulated in the manipulability denoted by m_1 , and m_2 .

$$\dot{q} = J(q)^{-1} \nu. \quad (3)$$

Note that the t variable in (3) has been omitted for clarity. (3) can only be solved when $J(q)$ is square (and non-singular), which is when the robot has 6 degrees-of-freedom.

For redundant robots there is no unique solution for (2). Consequently, the most common solution to this is to use the Moore-Penrose pseudoinverse

$$\dot{q} = J(q)^+ \nu. \quad (4)$$

where the $(\cdot)^+$ denotes the pseudoinverse operation. The pseudoinverse will find ν with the minimum Euclidean norm, which is useful for a real robot.

IV. QUADRATIC PROGRAMMING

A general constrained quadratic programming (QP) problem is formulated as [5]

$$\begin{aligned} \min_x \quad & f_o(x) = \frac{1}{2} x^\top Q x + c^\top x, \\ \text{subject to} \quad & A_1 x = b_1, \\ & A_2 x \geq b_2. \end{aligned} \quad (5)$$

where $f_o(x)$ is the objective function which is subject to the following equality and inequality constraints. Typically, at least one constraint needs to be defined. A quadratic program is strictly convex when the matrix Q is positive definite [5].

Equation (4) can be reformulated as a constrained quadratic programming problem in the form of (5)

$$\begin{aligned} \min_{\dot{q}} \quad & f_o(\dot{q}) = \frac{1}{2} \dot{q}^\top I_n \dot{q}, \\ \text{subject to} \quad & J(q) \dot{q} = \nu \end{aligned} \quad (6)$$

where I_n is an $n \times n$ identity matrix, and no inequality constraints need to be defined.

This optimisation minimises the control input, which in this case is joint velocities. Joint torque is not considered.

V. THE MANIPULABILITY JACOBIAN

A. The Manipulability Measure

A notable problem arises in serial-link manipulators when they approach a kinematic singularity. The kinematic Jacobian becomes ill-conditioned and the robot can not move easily within its workspace. This can cause required joint velocities to approach impossible levels [4]. Additionally, at the singularity, the robot's task space is reduced by one or more degrees of freedom.

The manipulability measure in [1], describes how well-conditioned the manipulator is to achieve an arbitrary velocity. It is a scalar

$$m = \sqrt{\det(J(q)J(q)^\top)} \quad (7)$$

which describes the volume of a 6-dimensional ellipsoid defined by

$$J(q)J(q)^\top. \quad (8)$$

If this ellipsoid has a large volume and is close to spherical, then the manipulator can achieve any arbitrary end-effector velocity. A 6-dimensional ellipsoid is impossible to display, but the first three rows of the kinematic Jacobian represent the translational component of the end-effector velocity and the last three rows represent the end-effector angular velocity. Therefore, by using only the first or last three rows of a kinematic Jacobian in (8), the 3-dimensional translation or angular velocity ellipsoids respectively can be found and visualised. For example, Figure 2 show two angular velocity ellipsoids for two different robot configurations.

The ellipsoid has three radii, along its principle axes. A small radius along an axis represents the robots inability to achieve a velocity in the corresponding direction. At a

singularity, the ellipsoid's radius becomes zero along the corresponding axis. Therefore the volume becomes zero. If the manipulator's configuration is well conditioned, these ellipsoids will have a larger volume. Additionally, the manipulability translational m_t or rotational m_r components respectively can be found by taking the first, or last three rows of the manipulator Jacobian to calculate (7).

Therefore, the manipulability presents a favourable performance index for an optimisation function. However, it has a highly non-linear relationship with the manipulator's joint coordinates. Consequently, just as we use the kinematic Jacobian in (2) to relate the joint velocities to the end-effector velocities, we can derive a manipulability Jacobian to relate the joint velocities to the rate of change of the manipulability.

B. The Manipulability Jacobian

Taking the time derivative of (7), using the chain rule

$$\frac{d m(t)}{dt} = \frac{1}{2m(t)} \frac{d \det(\mathbf{J}(\mathbf{q})\mathbf{J}(\mathbf{q})^\top)}{dt} \quad (9)$$

and simply yields

$$\dot{m} = \mathbf{M}^\top \dot{\mathbf{q}} \quad (10)$$

where

$$\mathbf{M} = \begin{pmatrix} m \text{vec}(\mathbf{J}\mathbf{H}_1^\top)^\top \text{vec}((\mathbf{J}\mathbf{J}^\top)^{-1}) \\ m \text{vec}(\mathbf{J}\mathbf{H}_2^\top)^\top \text{vec}((\mathbf{J}\mathbf{J}^\top)^{-1}) \\ \vdots \\ m \text{vec}(\mathbf{J}\mathbf{H}_n^\top)^\top \text{vec}((\mathbf{J}\mathbf{J}^\top)^{-1}) \end{pmatrix} \quad (11)$$

is the manipulability Jacobian with $\mathbf{M}^\top \in \mathbb{R}^n$ and where the vector operation $\text{vec}(\cdot) : \mathbb{R}^{a \times b} \rightarrow \mathbb{R}^{ab}$ vectorises a matrix into a vector, and $\mathbf{H}_i \in \mathbb{R}^{6 \times n}$ is the i^{th} component of the manipulator Hessian $\mathbf{H} \in \mathbb{R}^{6 \times n \times n}$. We provide a full derivation of the manipulability Jacobian in Appendix I.

VI. MANIPULABILITY MOTION CONTROLLER DESIGN

We use the manipulability Jacobian from (11) as the main term to optimise over in a quadratic program. Recalling the general form of a quadratic program from (5), the equation for the derivative of the manipulability in (10) fits the form of the linear component of the quadratic program. While we could end the controller here as a linear program, optimisers will likely yield unreasonable or dangerous control inputs to the system if the control input is not penalised [5]. Hence, we keep the basic quadratic programming form of the pseudoinverse and augment it to also maximise the manipulability. Therefore, the final optimisation problem is

$$\begin{aligned} \min_{\dot{\mathbf{q}}} \quad & f_o(\dot{\mathbf{q}}) = \frac{1}{2} \dot{\mathbf{q}}^\top \lambda \mathbf{I}_n \dot{\mathbf{q}} - \mathbf{M}^\top \dot{\mathbf{q}}, \\ \text{subject to} \quad & \mathbf{J} \dot{\mathbf{q}} = \mathbf{v}. \end{aligned} \quad (12)$$

where $\lambda \in \mathbb{R}^+$ is a gain term, and we use $-\mathbf{M}$ to maximize rather than minimize manipulability. Since $\lambda \mathbf{I}_n$ is positive definite, the resulting optimisation problem is convex. The gain term λ can be adjusted to tune how much the controller will minimise the control input relative to maximising the manipulability. If desired, an inequality constraint can be added to (12) which will bind the joint velocities speeds

$$\begin{aligned} \text{subject to} \quad & \mathbf{I}_n \dot{\mathbf{q}} \leq \boldsymbol{\alpha}, \\ & \mathbf{I}_n \dot{\mathbf{q}} \geq -\boldsymbol{\alpha} \end{aligned}$$

where $\boldsymbol{\alpha} \in \mathbb{R}^n$ is a vector representing the maximum joint speed for each joint.

We use the algorithm and Python library from [17] to calculate the kinematic Jacobian, and Hessian required for the manipulability Jacobian. Furthermore, we extend this Python library to calculate the manipulability Jacobian and implement the manipulability maximising resolved-rate motion controller in (12). We use the Python library qpsolvers which implements the quadratic programming solver devised in [18] to optimise (12). We have released our implementation as an open-source Python library. The library requires only the standard or modified DenavitHartenberg parameters of the serial-link manipulator.

VII. EXPERIMENTS

We validate and evaluate our controller through testing on a real manipulator as well as in simulation on several different manipulators. We compare our Manipulability Motion Controller (MMC) to a standard Resolved-Rate Motion Controller (RRMC), which is the current standard for reactive velocity control of a robot's end-effector. In each experiment, we choose an initial joint configuration and an end-effector goal pose. A spatial velocity is computed to move from start to goal, and we capture the performance of MMC and RRMC for this motion.

The experiments are completed by having each controller operate a position-based servoing scheme in which both robots have the same initial joint configuration and end-effector pose, and finish with the same end-effector pose (but not necessarily the same joint configuration).

The position-based servoing (PBS) scheme is

$$\nu_e = k (({}^0\mathbf{T}_e)^{-1} \bullet {}^0\mathbf{T}_{e*}) \quad (13)$$

where k is a gain term, ${}^0\mathbf{T}_e \in \mathbf{SE}(3)$ is the end-effector pose in the robot's base frame, ${}^0\mathbf{T}_{e*} \in \mathbf{SE}(3)$ is the desired end-effector pose in the robot's base frame, and \bullet represents composition. This scheme will cause the robot's end-effector follow a straight path, in the robot's task space, to the goal pose.

We set $\lambda = 0.005$ in (12) for all experiments. This was found to provide a good balance between manipulability maximisation and control input minimisation.

TABLE I: Experiment 2: Results on 1000 Simulated PBS Tasks

Robot	Mean Manipulability			Mean Final Manipulability		
	RRMC	MMC (ours)	Improvement	RRMC	MMC (ours)	Improvement
Panda	0.0742	0.0880	18.6%	0.0782	0.0934	19.6%
LBR-7	0.0667	0.0776	16.4%	0.0643	0.0761	18.5%
Sawyer	0.2721	0.3206	17.8%	0.2572	0.3263	26.8%

A. Simulation Components

For the simulated experiments, we use our open-source Python library, and PyRep [19] with CoppeliaSim to simulate several robots: the Franka-Emika Panda, the Rethink Sawyer, and the Kuka LBR iiwa 7 R800 (LBR-7). All robots have 7 DoF.

B. Experiment 2: Simulated Robots

We compare our MMC to RRMC by having them operate the PBS scheme in (13) between 1000 randomly generated poses on each simulated serial-link manipulator. This experiment shows how much the MMC improves manipulability on average in a large scale test. We provide the results in Table I.

The initial configuration of the robot is generated by choosing random joint angles for each joint in the robot

$$q_i = \text{rand}(q_{i \min} + 50^\circ, q_{i \max} - 50^\circ) \quad (14)$$

where $q_{i \min}$ and $q_{i \max}$ are the minimum and maximum valid joint angles (as specified by the manufacturer) for the joint q_i , the function $\text{rand}(a, b)$ returns a uniformly distributed number between a and b , and the 50° offset is used to assist in keeping the configurations away from singular positions and self collisions. Configurations which result in self collisions are discarded.

The final pose is generated using (14) and using the forward kinematics of the robot to calculate the pose of the robot in that configuration. This pose is then used as ${}^0T_{e^*}$ in (13).

C. Physical Components

For the physical experiments, we use our open-source Python library and ROS middleware to interface with the robot. We use the 7 degree-of-freedom Franka-Emika Panda robot in these experiments.

D. Experiment 1: Physical Robot

We compare MMC and RRMC by having them operate the PBS scheme in (13) for several different scenarios. These scenarios reflect common operational situations which the controllers can encounter.

- Both controllers servo between two poses in which the robot is well conditioned and not near a singularity. This reflects average and non-extreme operation of the robot. Furthermore, this is likely to be the most common scenario for a servo controller.
- Both controllers servo between two poses which differ greatly in orientation. In this experiment, the robot's

end-effector starts facing the ground and finishes facing the sky. This reflects an extreme operation of the robot.

- Both controllers servo from a pose in which the robot is close to singularity and poorly conditioned to a pose in which the robot is well-conditioned. This experiment shows how each controller recovers the robot from a difficult pose.
- Both controllers servo from a pose in which the robot is well conditioned to a pose in which the robot is close to a singularity. In this experiment, the robot's final pose is on the outer bounds of the robot's task space. This experiment shows how the controllers behave when the robot moves towards a singular position.

VIII. RESULTS

Our experiments show that the proposed MMC significantly improves the manipulability of a manipulator when compared to RRMC, while velocity controlling the end-effector.

The average execution time of the MMC controller during the experiments was 0.00826 s. This was using an Intel i7-8700K CPU with 12 cores at 3.70GHz. Therefore, the MMC controller can comfortably run within a 100 Hz control loop. Reducing the execution time is possible through using multi-threading techniques as the program is easily parallelizable.

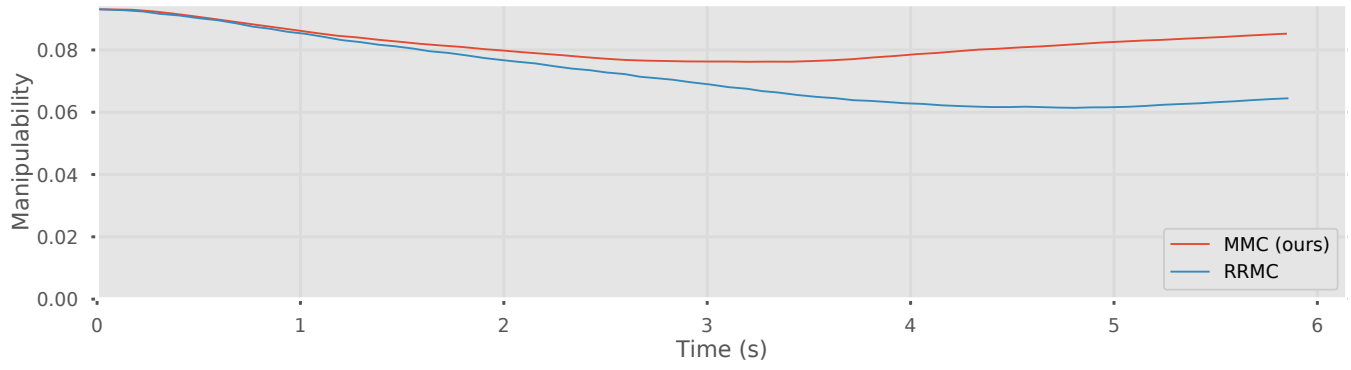
A. Simulation Results

Experiment 2 shows how MMC improves the general manipulability on different manipulators when compared to RRMC. The results, displayed in Table I show that MMC provides 18% better manipulability on average when exhaustively tested on three different 7 DoF manipulators. Furthermore, MMC improves the final manipulability by 22% on average. This shows that the general performance of MMC far outperforms RRMC.

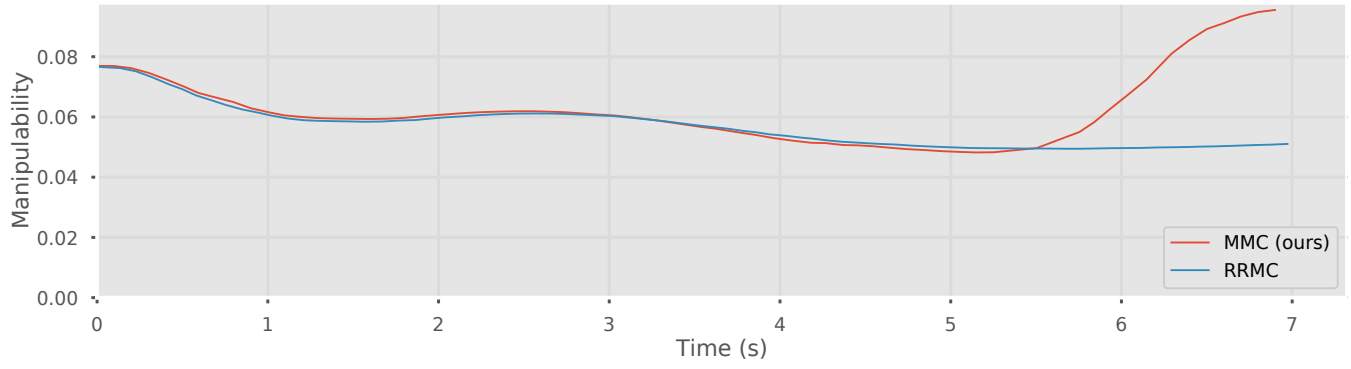
B. Physical Results

Figure 3a shows how the controller improves the manipulability during a normal servoing operation. This figure shows that the MMC slowly improves the manipulability as the robot approaches the final pose. This scenario reflects the most common operation of the robot and shows that the MMC can improve manipulability on simple servoing tasks.

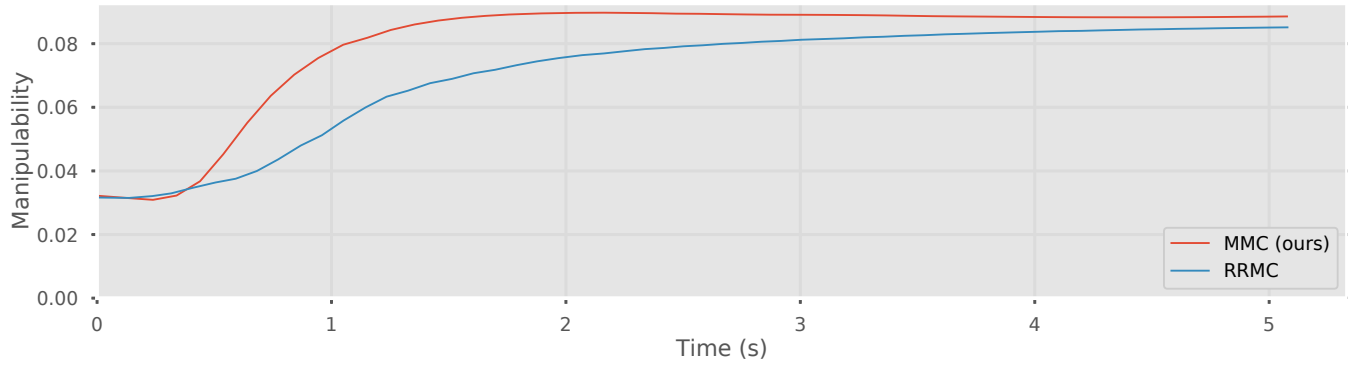
Figure 3b shows that during a complex servoing operation, MMC causes the robot to enter a configuration which improves the manipulability greatly. When the robot performs a complex movement, RRMC, which minimises the total joint velocity, can cause the robot to become *twisted up*. This



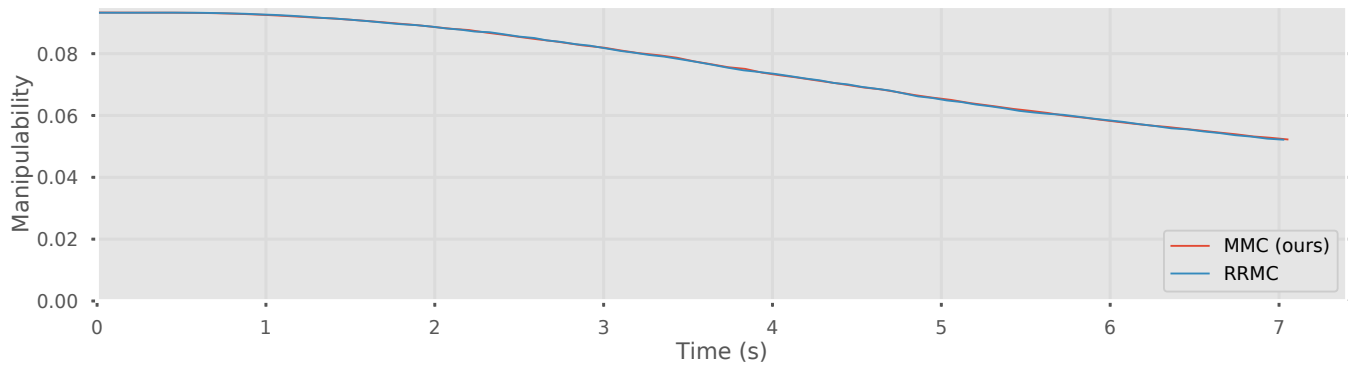
(a) Robot Manipulability Measure during a Normal Servo Operation



(b) Robot Manipulability Measure during a Complex Servo Operation



(c) Robot Manipulability Measure with the Robot's Initial Position near a Singularity



(d) Robot Manipulability Measure with the Robot's Final Pose near a Singularity

Fig. 3: Experiment 1: Robot Manipulability Measure of RRMC and MMC during PBS in Various Scenarios

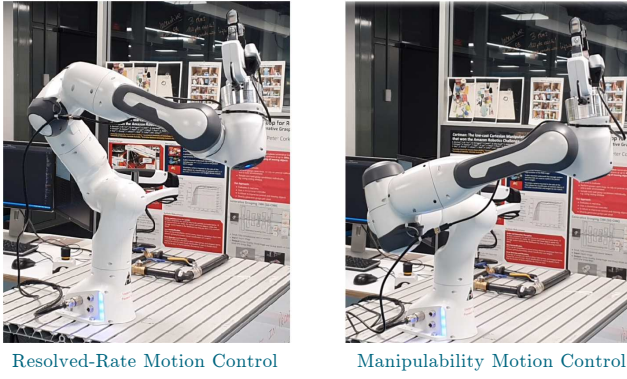


Fig. 4: Final Pose of Experiment 1b: MMC provides a final pose which has 50% better manipulability than RRMC.

means that robots links are in close proximity and causes the robot to be poorly conditioned. MMC, as shown in Figure 3b, unravels the robot after the complicated movement to finish in a far superior configuration. Figure 4, displays the difference in final pose for this experiment.

Figure 3c and 3d show edge cases of the robot recovering from a difficult configuration and entering a difficult configuration respectively. Figure 3c shows that MMC assists the robot in recovering from a poorly conditioned configuration much faster than RRMC, and reaches a larger final manipulability. Figure 3d, shows the manipulability of the robot as it completes a reaching task where the final pose is on the outer bounds of the robot's task space. In this situation, there is no room for improvement in manipulability as the robot is fully outstretched. Consequently, both MMC and RRMC exhibit the same manipulability throughout the experiment. This shows that the worst-case performance of MMC is that it will generate the same control output as RRMC.

A limitation of our approach is that it is more complex to implement than RRMC. However, to mitigate this, we have produced an open-source Python implementation which calculates all required components of MMC including the manipulability Jacobian, the kinematic Jacobian, and the kinematic Hessian. The only required input for our library to work is the standard or modified DenavitHartenberg parameters of the manipulator, and the joint angles.

IX. CONCLUSIONS

In this paper we have presented our Manipulability Motion Controller (MMC) as an improved resolved-rate motion controller for redundant manipulators. The existing solution to resolved-rate motion control uses a simplistic minimum norm solution for redundancy resolution, while our MMC also maximises the manipulability of the manipulator. Our results show our approach operating in several different scenarios on a real robot, and improve the average manipulability by 19% for a Panda robot, 16% on an LBW-7 Robot, and 18% on a Sawyer robot, in a large scale simulation. This translates to greatly improved robustness in the operation manipulators in a purely reactive manner.

REFERENCES

- [1] T. Yoshikawa, "Manipulability of Robotic Mechanisms," *The International Journal of Robotics Research*, vol. 4, no. 2, pp. 3–9, 1985.
- [2] D. E. Whitney, "Resolved motion rate control of manipulators and human prostheses," *IEEE Transactions on Man-Machine Systems*, vol. 10, no. 2, pp. 47–53, June 1969.
- [3] Gu Ming Kun, Wang Dan Wei, and Soh Yeng Chai, "A fuzzy logic approach for kinematic control of redundant manipulators," in *Proceedings 1993 Asia-Pacific Workshop on Advances in Motion Control*, July 1993, pp. 94–99.
- [4] P. Corke, *Robotics, Vision and Control*, 2nd ed. Springer International Publishing, 2017.
- [5] J. Nocedal and S. Wright, *Numerical optimization*. Springer Science & Business Media, 2006.
- [6] J. M. Ahuactzin and K. K. Gupta, "The kinematic roadmap: a motion planning based global approach for inverse kinematics of redundant robots," *IEEE Transactions on Robotics and Automation*, vol. 15, no. 4, pp. 653–669, Aug 1999.
- [7] D. Guo, F. Xu, and L. Yan, "New pseudoinverse-based path-planning scheme with pid characteristic for redundant robot manipulators in the presence of noise," *IEEE Transactions on Control Systems Technology*, vol. 26, no. 6, pp. 2008–2019, Nov 2018.
- [8] D. Guo and Y. Zhang, "Acceleration-level inequality-based man scheme for obstacle avoidance of redundant robot manipulators," *IEEE Transactions on Industrial Electronics*, vol. 61, no. 12, pp. 6903–6914, Dec 2014.
- [9] Y. Zhang, X. Yan, D. Chen, D. Guo, and W. Li, "Qp-based refined manipulability-maximizing scheme for coordinated motion planning and control of physically constrained wheeled mobile redundant manipulators," *Nonlinear Dynamics*, vol. 85, no. 1, pp. 245–261, 07 2016.
- [10] L. Jin, S. Li, H. M. La, and X. Luo, "Manipulability optimization of redundant manipulators using dynamic neural networks," *IEEE Transactions on Industrial Electronics*, vol. 64, no. 6, pp. 4710–4720, June 2017.
- [11] D. Guo and Y. Zhang, "Li-function activated ZNN with finite-time convergence applied to redundant-manipulator kinematic control via time-varying Jacobian matrix pseudoinversion," *Applied Soft Computing*, vol. 24, pp. 158–168, 2014.
- [12] B. Cai and Y. Zhang, "Different-level redundancy-resolution and its equivalent relationship analysis for robot manipulators using gradient-descent and zhang 's neural-dynamic methods," *IEEE Transactions on Industrial Electronics*, vol. 59, no. 8, pp. 3146–3155, Aug 2012.
- [13] S. Li, Y. Zhang, and L. Jin, "Kinematic control of redundant manipulators using neural networks," *IEEE Transactions on Neural Networks and Learning Systems*, vol. 28, no. 10, pp. 2243–2254, Oct 2017.
- [14] Y. S. Xia, Gang Feng, and Jun Wang, "A primal-dual neural network for online resolving constrained kinematic redundancy in robot motion control," *IEEE Transactions on Systems, Man, and Cybernetics, Part B (Cybernetics)*, vol. 35, no. 1, pp. 54–64, Feb 2005.
- [15] S. Hutchinson, G. D. Hager, and P. I. Corke, "A tutorial on visual servo control," *IEEE Transactions on Robotics and Automation*, vol. 12, no. 5, pp. 651–670, Oct 1996.
- [16] D. J. Agravante, G. Claudio, F. Spindler, and F. Chaumette, "Visual servoing in an optimization framework for the whole-body control of humanoid robots," *IEEE Robotics and Automation Letters*, vol. 2, no. 2, pp. 608–615, April 2017.
- [17] J. Haviland and P. Corke, "A systematic approach to computing the manipulator jacobian and hessian using the elementary transform sequence," *arXiv preprint*, 2020.
- [18] D. Goldfarb and A. Idnani, "A numerically stable dual method for solving strictly convex quadratic programs," *Mathematical programming*, vol. 27, no. 1, pp. 1–33, 1983.
- [19] S. James, M. Freese, and A. J. Davison, "Pyrep: Bringing v-rep to deep robot learning," *arXiv preprint arXiv:1906.11176*, 2019.
- [20] J. R. Magnus and H. Neudecker, *Matrix differential calculus with applications in statistics and econometrics*. John Wiley & Sons, 2019.

APPENDIX I

DERIVING THE MANIPULABILITY JACOBIAN

The manipulability Jacobian is obtained by taking the time derivative of (7) and applying the chain rule

$$\frac{d m(t)}{dt} = \frac{1}{2m(t)} \frac{d \det(\mathbf{J}(\mathbf{q})\mathbf{J}(\mathbf{q})^\top)}{dt} \quad (15)$$

where $\det(\mathbf{J}(\mathbf{q})\mathbf{J}(\mathbf{q})^\top)$ is a scalar function of a vector. Jacobi's formula expresses the derivative of the determinant of a matrix [20]

$$\begin{aligned} \frac{d \det(\mathbf{A}(x))}{dx} &= \text{tr} \left(\text{adj}(\mathbf{A}(x)) \frac{d\mathbf{A}(x)}{dx} \right) \\ &= \det(\mathbf{A}(x)) \text{tr} \left(\mathbf{A}(x)^{-1} \frac{d\mathbf{A}(x)}{dx} \right) \end{aligned} \quad (16)$$

where $\text{adj}(\mathbf{A}) = \det(\mathbf{A})\mathbf{A}^{-1}$ is the adjugate of a matrix, and $\text{tr}(\cdot)$ is the trace of a matrix. Using (16) to expand the rightmost term of (15) gives

$$\frac{d(\det(\mathbf{J}\mathbf{J}^\top))}{dt} = \det(\mathbf{J}\mathbf{J}^\top) \text{tr} \left((\mathbf{J}\mathbf{J}^\top)^{-1} \frac{d\mathbf{J}\mathbf{J}^\top}{dt} \right). \quad (17)$$

Additionally, using the product rule to expand the remaining derivative in (17)

$$\frac{d(\det(\mathbf{J}\mathbf{J}^\top))}{dt} = \det(\mathbf{J}\mathbf{J}^\top) \text{tr} \left((\mathbf{J}\mathbf{J}^\top)^{-1} (\dot{\mathbf{J}}\mathbf{J}^\top + \mathbf{J}\dot{\mathbf{J}}^\top) \right)$$

where $\dot{\mathbf{J}}$ is the time derivative of \mathbf{J} . Using the property $(\mathbf{J}^\top)^\top = (\dot{\mathbf{J}})^\top$, the trace product property, and the trace cyclic property, this can be simplified to

$$\begin{aligned} \frac{d(\det(\mathbf{J}\mathbf{J}^\top))}{dt} &= \det(\mathbf{J}\mathbf{J}^\top) \times \\ &\quad \text{tr} \left(\dot{\mathbf{J}}\mathbf{J}^\top (\mathbf{J}\mathbf{J}^\top)^{-1} + \mathbf{J}\mathbf{J}^\top (\dot{\mathbf{J}}\mathbf{J}^\top)^{-1} \right) \\ &= 2 \det(\mathbf{J}\mathbf{J}^\top) \text{tr} \left(\dot{\mathbf{J}}\mathbf{J}^\top (\mathbf{J}\mathbf{J}^\top)^{-1} \right). \end{aligned} \quad (18)$$

Substituting (18) back into (15) yields

$$\begin{aligned} \dot{m} &= \frac{1}{2m(t)} 2 \det(\mathbf{J}\mathbf{J}^\top) \text{tr} \left(\dot{\mathbf{J}}\mathbf{J}^\top (\mathbf{J}\mathbf{J}^\top)^{-1} \right) \\ &= \sqrt{\det(\mathbf{J}\mathbf{J}^\top)} \text{tr} \left(\dot{\mathbf{J}}\mathbf{J}^\top (\mathbf{J}\mathbf{J}^\top)^{-1} \right) \\ &= m \text{tr} \left(\dot{\mathbf{J}}\mathbf{J}^\top (\mathbf{J}\mathbf{J}^\top)^{-1} \right) \end{aligned} \quad (19)$$

where m is defined in (7), and $\dot{\mathbf{J}}$ is the time derivative of the manipulator Jacobian. Using the chain rule, (19) becomes

$$\begin{aligned} \frac{d \mathbf{J}(\mathbf{q}(t))}{dt} &= \frac{\partial \mathbf{J}(\mathbf{q})}{\partial \mathbf{q}} \frac{d\mathbf{q}(t)}{dt} \\ &= \sum_{i=1}^n \frac{\partial \mathbf{J}(\mathbf{q})}{\partial q_i} \dot{q}_i \\ &= \sum_{i=1}^n \mathbf{H}_i(\mathbf{q}) \dot{q}_i \\ &= \mathbf{H}(\mathbf{q}) \dot{\mathbf{q}} \end{aligned} \quad (20)$$

where $\mathbf{H}(\mathbf{q}) \in \mathbb{R}^{6 \times n \times n}$ is the manipulator Hessian. Substituting the result from (20) into (19) we obtain

$$\begin{aligned} \dot{m} &= m \text{tr} \left(\left(\sum_{i=1}^n \mathbf{H}_i \dot{q}_i \right) \mathbf{J}^\top (\mathbf{J}\mathbf{J}^\top)^{-1} \right) \\ &= m \sum_{i=1}^n \left(\dot{q}_i \text{tr} \left(\mathbf{H}_i \mathbf{J}^\top (\mathbf{J}\mathbf{J}^\top)^{-1} \right) \right). \end{aligned} \quad (21)$$

Using the relationship $\mathbf{B}^\top \mathbf{A}^\top = (\mathbf{A}\mathbf{B})^\top$, (21) becomes

$$\dot{m} = m \sum_{i=1}^k \left(\dot{q}_i \text{tr} \left((\mathbf{J}\mathbf{H}_i^\top)^\top (\mathbf{J}\mathbf{J}^\top)^{-1} \right) \right). \quad (22)$$

Furthermore, using the relationship

$$\text{tr}(\mathbf{A}^\top \mathbf{B}) = \text{vec}(\mathbf{A})^\top \text{vec}(\mathbf{B}),$$

where the vector operation $\text{vec}(\cdot) : \mathbb{R}^{a \times b} \rightarrow \mathbb{R}^{ab}$ vectorises a matrix into a vector, (22) becomes

$$\begin{aligned} \dot{m} &= m \sum_{i=1}^n \left(\dot{q}_i \text{vec} \left(\mathbf{J}\mathbf{H}_i^\top \right)^\top \text{vec} \left((\mathbf{J}\mathbf{J}^\top)^{-1} \right) \right) \\ &= \sum_{i=1}^n \left(\dot{q}_i m \text{vec} \left(\mathbf{J}\mathbf{H}_i^\top \right)^\top \text{vec} \left((\mathbf{J}\mathbf{J}^\top)^{-1} \right) \right) \\ &= \begin{pmatrix} \dot{q}_1 & \dots & \dot{q}_n \end{pmatrix} \begin{pmatrix} m \text{vec} \left(\mathbf{J}\mathbf{H}_1^\top \right)^\top \text{vec} \left((\mathbf{J}\mathbf{J}^\top)^{-1} \right) \\ m \text{vec} \left(\mathbf{J}\mathbf{H}_2^\top \right)^\top \text{vec} \left((\mathbf{J}\mathbf{J}^\top)^{-1} \right) \\ \vdots \\ m \text{vec} \left(\mathbf{J}\mathbf{H}_n^\top \right)^\top \text{vec} \left((\mathbf{J}\mathbf{J}^\top)^{-1} \right) \end{pmatrix} \\ &= \dot{\mathbf{q}}^\top \mathbf{M} \\ &= \mathbf{M}^\top \dot{\mathbf{q}} \end{aligned} \quad (23)$$

where

$$\mathbf{M} = \begin{pmatrix} m \text{vec} \left(\mathbf{J}\mathbf{H}_1^\top \right)^\top \text{vec} \left((\mathbf{J}\mathbf{J}^\top)^{-1} \right) \\ m \text{vec} \left(\mathbf{J}\mathbf{H}_2^\top \right)^\top \text{vec} \left((\mathbf{J}\mathbf{J}^\top)^{-1} \right) \\ \vdots \\ m \text{vec} \left(\mathbf{J}\mathbf{H}_n^\top \right)^\top \text{vec} \left((\mathbf{J}\mathbf{J}^\top)^{-1} \right) \end{pmatrix} \quad (24)$$

is the manipulability Jacobian with $\mathbf{M}^\top \in \mathbb{R}^n$.